Surface Enhanced Raman Scattering Effects of Silver Colloids with Different Shapes

Jiatao Zhang, Xiaolin Li, Xiaoming Sun, and Yadong Li*

Department of Chemistry, Tsinghua University, Beijing, 100084, P. R. China, and National Center for Nanoscience and Nanotechnology, Beijing, 100084, P. R. China

Received: January 26, 2005; In Final Form: April 11, 2005

By solution-based method, three kinds of silver colloids, self-assembled nanowires, triangular nanoplates and quasispherical nanoparticles, have been synthesized. TEM studies revealed that they exposed different crystal planes, such as {111} crystal planes to triangular nanoplates, mainly {100} and {111} planes to self-assembly nanowires. Hereby, do the distinct shapes and crystal planes have an impact on the surface enhanced Raman scattering (SERS)? The great differences of the SERS spectra of rhodamine B at these Ag colloids confirmed that the shapes and crystal planes of silver have great effect on Raman enhancement, especially the crystal planes.

1. Introduction

The discovery of surface enhanced Raman scattering (SERS) has great importance on the surface science and spectroscopy because of its extremely high sensitivity and the extensive applications in electrochemistry, analysis, and biology. Since the discovery of this phenomenon from pyridine absorbed on an electrochemically roughened silver electrode reported by Fleischmann in 1974,[1] many researchers have been working in the field of SERS to explore the basic nature of it and to apply this new technique to surface science, trace analysis, and sensing.[2−6] The most progress that should be mentioned is the single molecule detection found by Nie, Kneipp, etc., and the enhancement factor can be as high as $10^{14}-10^{15}$ on a single Ag nanoparticle. Nie and co-workers also have researched the Ag size effect and obtained the result of size-dependent optical enhancement and surface activation.[7−8] To find more SERS-active substrates, Tian etc. used the electrochemical etching method to obtain transition-metal Pt, Rh, Fe, Ni, and Co electrodes which have good SERS activities.[9] Recently, Zhang etc. found the gold nanoparticle aggregate (GNA) system was highly active to SERS, which could yield enhancement of $10^{7}-10^{9}$ for R6G, and also had good activity on biomolecular detection due to strong near-IR absorption of the GNA.[10]

Up until now, what had been widely admitted was two enhancement mechanisms, one being the long-range electromagnetic (EM) effect and the other the short-range chemical (CHEM) effect, which were simultaneously operative. The EM mechanism, contributing a large part to the overall enhancement factor (EF), is based on the amplified electromagnetic field generated upon optical excitation of surface plasma resonance of nanoscale surface roughness features in the 10−100 nm range.[11] Furthermore, many theoretical models and experiments have shown that nanotip provides not only the large local field enhancement but also the high spatial resolution since most of the SERS signal is generated from the tip area. Thus the nanoshapes of SERS substrates must be very important to the SERS activity.[12−14] The CHEM enhancement mechanism is associated with the electronic coupling of molecules adsorbed on certain surface sites in atomic-scale roughness (such as atomic clusters, terraces, and steps), leading to the charge transfer between analyte and metal surface. So far, the widely accepted mechanism of CHEM is charge transfer theory and "hot site" theory.[7b,10b,15] However, the radical reason for this chemical effect has not been understood. Thus to find the true mechanism of chemical interaction now becomes urgent.

Considering the CHEM effect, analogous to the heterogeneous catalysis, both involved the interaction process between absorbed molecules and the solid surface. And as we all know that the crystal plane of the semiconductor oxide catalyst plays an essential role in determining its catalytic oxidation properties, catalysts with well-defined reactive sites may be "designed" by morphology-controlled synthesis of nanostructured materials.[16] One question appears: whether different exposed crystal planes of nanometal surface have influence on the SERS activity. Consequently, in this paper, we have prepared three kinds of Ag with well-defined nanostructured surfaces and made a comparison on SERS spectra of rhodamine B molecules absorbed on them to explore the influence of the shape and the exposed crystal planes on the SERS enhancement.

2. Experimental Section

2.1. Chemicals and Materials. Anhydrous ethylene glycol (EG, 99.8%), silver nitrate ($AgNO_3$, 99+%), and poly(vinyl pyrrolidone) (PVP, MW = 1 300 000, MW = 40 000) were purchased from Beijing Chemical Reagent Co., Ltd. All chemicals were analytical grade and were used without further purification. Polished silicon (100) wafers were obtained from GRINM Semiconductor Materials Co., Ltd, Beijing.

2.2. Preparation of Silver Nanowires and Nanoparticles. The synthesis of silver nanowires and nanoparticles has been reported previously.[17,18] Briefly, 3 mL of an ethylene glycol (EG) solution of 0.25 M $AgNO_3$ and 3 mL of an EG solution of PVP (0.375 M in repeating unit, MW = 1 300 000) were mixed uniformly with stirring under room temperature. The mixture was then injected dropwise into 5 mL of EG, which had been previously refluxed at 160 °C for about 1 h. Then the reaction was continued at 160 °C for 60 min with vigorous magnetic stirring. The silver nanowires were separated from particles through centrifugation at 2000 rpm for ∼20 min and

* To whom all correspondence should be addressed at Tsinghua University. E-mail: ydli@tsinghua.edu.cn. Phone: 86-10-62772350. Fax: 86-10-62788765.

10.1021/jp050471d CCC: $30.25
Published on Web 06/04/2005

then wash 4−5 times with alcohol and acetone. The nanoparticles were made by changing the molar ratio of PVP and $AgNO_3$ to 6:1 and using PVP (MW = 40 000), and the samples were washed 4−5 times with alcohol and acetone.

2.3. Preparation of Silver Triangular Nanoplates. The silver triangular nanoplates were prepared by a solution-based solvothermal method with *N*,*N*-dimethylformamide (DMF) as a solvent and as a reducing agent.[19] In a typical synthesis, 20 mL of a DMF solution of 0.025 M $AgNO_3$ was added dropwise into 20 mL of a DMF solution of 0.075 M PVP (MW = 40 000) until the mixture turned orange, then the solution was transferred into a 50-mL autoclave and heated at 150 ∼180 °C under autogenetic pressure for 24 h. The final sample was obtained by centrifugation at 4500 rpm and washing 4−5 times with acetone and alcohol.

2.4. Characterization. The Ag substrates were prepared by putting the Ag-alcohol colloids on an n-Si (100) wafer for SEM and SERS tests. The SEM images of Ag substrates were obtained with a JSM-6301F field-emission microscope, and TEM and SAED investigations were performed with a JEM-1200EX microscope operated at 120 KV. An X-ray diffraction test was performed with a Bruker D8 Advance X-ray diffractometer with monochromatized Cu Kα radiation (λ = 1.5418 Å). The UV−vis spectra were obtained with use of UV-3101 by a Hitachi U-3010 spectrophotometer. Before SERS measurements, three Ag substrates were each dipped in a 3 mL solution of rhodamine B (10^{-8} M, in water) for 30 min then dried at 60 °C for 1 h. The SERS spectra were recorded with a microscopic confocal Raman spectrometer (model RM 2000, Renishaw PLC, England), using a laser beam with an excitation wavelength of 514 nm and a charge-coupled device (CCD) detector with a resolution of 4 cm^{-1}. The power was maintained very low (∼0.47 mW) to avoid destruction of the samples.

3. Results and Discussion

3.1. Crystal Planes and Morphologies Analysis. Figure 1 shows the SEM and TEM images of as-prepared Ag nanowires, triangular nanoplates, and nanoparticles. Figure 1A is the morphology of the nanowire substrate for the SERS test. As shown in the figure, the nanowires are uniformly ∼100 nm in diameter and can be self-assembled to obtain a well-ordered local domain although a long-range order cannot be formed. Fortunately it has been enough for microscopic confocal Raman research. This self-assembly process may be due to the entropy-driven force with the evaporation of alcohol when putting the colloid on the Si wafer.[18a,20] Figure 1B shows the individual nanowire TEM image and SAED pattern. From the electric diffraction analysis, the reflection assignments agreed well with the results of Ag nanowires reported previously. So we can affirm the Ag nanowires prepared here have a 5-fold twinned structure bounded by five {100} side planes and capped by five {111} planes with [110] growth direction, as shown below in Figure 1B.[17b,18a] Figure 1C shows the triangular plates for the SERS test. As shown in the figure, the as-prepared triangular nanoplates mostly have sharp tips and smooth fringes. From the inset we can see the clear shapes of as-prepared triangular nanoplates. Figure 1D is the TEM image of as-prepared silver plates and the corresponding SAED pattern. From the SAED pattern, we can confirm each nanoplate is a single crystal bounded by triangular {111} facets.[17c] Figure 1E is the image of the silver particle substrate for the SERS test. Figure 1F shows the TEM image of as-obtained silver nanoparticles. From Figure 1E,F, it is obvious that the size is 100−300 nm, nearly the same as that of nanoplates. The particles have random shapes, such as truncated tetrahedral and some other polyhedrons. Owing to randomicity and complexity of the as-prepared particle shapes, the exposure of all silver crystal planes is possible, which agrees well with Prywer's theory of crystal growth, [21]such as {111}, {100}, {110}, and {311} crystal planes.

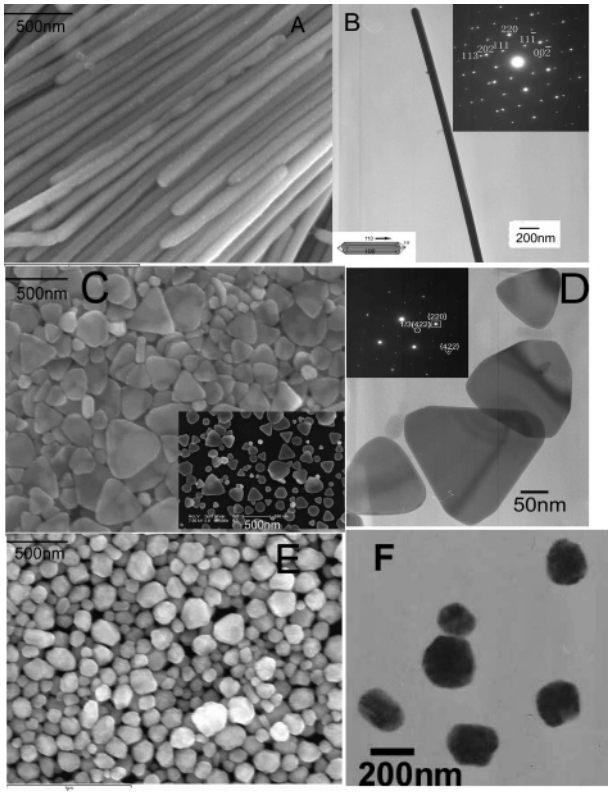

Figure 1. (A) SEM image of self-assembled silver nanowires putting on Si wafer used for SERS detection; (B) TEM image of an individual Ag nanowire. The inset shows a structural model of the silver nanowires and the SAED pattern of a silver nanowire. (C) SEM image of a substrate for SERS detection with as-prepared silver triangular nanoplates. The inset below shows the clear shape of triangular plates. (D) TEM image of as-prepared Ag triangular nanoplates. The inset above shows the SAED image of a single nanoplate. The boxed spots could be indexed to the {220} reflections, the inner spot (circled) with a weak intensity corresponded to the forbidden 1/3 {422} reflections, the outer spot (triangled) should be assigned to the {422} reflections. (E) The SEM image of a silver particle substrate for SERS detection. (F) The TEM image of as-obtained Ag particles.

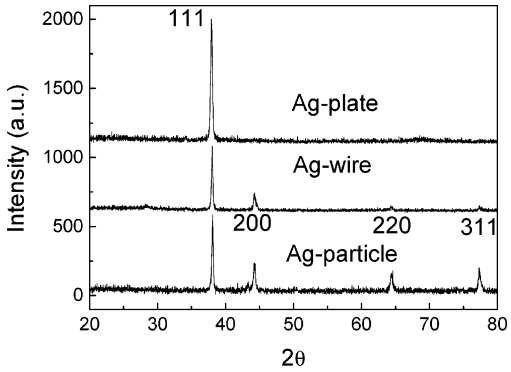

Figure 2. The XRD comparison of as-prepared Ag plate, Ag wire, and Ag particle.

To further identify the crystal structure of three kinds of silver substrate for the SERS test, the results of the XRD tests have been shown in Figure 2. From the XRD pattern, it is obvious that there is only one peak indexed as [111] peak to triangular plates and mainly two peaks attributed to [111] and [200] peaks

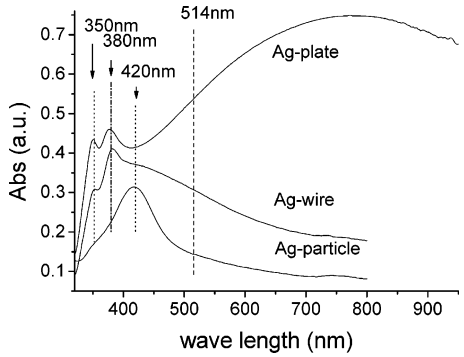

Figure 3. The UV−vis spectra comparison of three kinds of Ag samples obtained from their alcohol colloid.

to nanowires. Because the triangular plates are thin flakes (10−20 nm in thickness) and almost only the {111} facets are parallel to the Si substrate, then only the [111] peak appears in the XRD pattern.[17c] According to the crystal face growth rule put forward by Gilman, Brice etc., to reach the state of thermodynamic stability, the crystal face with high free energies should grow more quickly and be more difficult to expose in large proportions.[22] However, the crystal faces with low free energies can be exposed in large proportions, such as the {111} crystal face. Thus the crystal faces with higher surface free energies, such as {110} and {311} crystal faces, should more easily appear on edges, corners, protuberances, etc. in very small proportions. It is reasonable as-prepared nanopartilces show all the crystal planes of FCC silver, such as the [200], [220], and [311] peaks, probably because of their random polyhedron morphology.[21] All the results of XRD analysis agree well with the TEM measurements mentioned above and the reports previously.[17,18b,19a]

3.2. UV−Vis Absorption Spectra Analysis. Figure 3 shows the UV−vis spectra of three kinds of as-prepared Ag obtained from their alcohol colloids. It is clear that the shape has a great effect on the absorption peak. The nanoparticles have a plasmon peak at ∼420 nm. The nanowires mainly have two peaks attributing to the longitudinal mode (350 nm) and the transverse mode (380 nm) of surface plasma resonance.[17d] The surprising result is the absorption spectrum of as-prepared triangular nanoplates, which is a little different from the reported results. There are three parts of the peak, 350 nm, 380 nm, and a wide absorption in the visible region 600−900 nm. The 350 nm and 380 nm peaks should be attributed to the weak out-of-plane dipole and quadrupole resonance, respectively. As calculated before,[17c,19] the wide absorption in the visible region is due to the red shift of relatively intense in-plane dipole resonance because of the size distribution and the truncation degree of the angles. This can be identified by the SEM image in Figure 1C. Because of the strong surface plasma resonance around 780 nm, which is close to the laser excitation wavelength (e.g., 785 nm) of Raman spectroscopy, we expect that these particles should have promising usage in biomolecule detection by surface enhanced resonance Raman scattering (SERRS).[10b,23]

3.3. SERS Measurement and Discussions. From the above analysis of morphologies and surface optical properties, it is reasonable that these Ag substrates should have great differences on the SERS activities of organic molecules. Thus we used rhodamine B (10^{-8} mol/L) as absorbate to study the effects of the morphologies of as-obtained Ag substrates and the comparison of 10^{-8} M RhB with no silver enhancement shown in Figure 4A−D. The experimental Raman shifts, the comparison to the literature reports, and the assignments of these Raman shifts are listed in Table 1. From the comparison of Raman spectra of 10^{-8} M RhB, especially the inset quantitative intensity comparison in Figure 4A−C, we can see that the Raman enhancement of the Ag particle is better than that of the Ag wire and the Ag plate, and the Ag plate is worst. However, relative intensities of some Raman peaks show little difference, such as the 620 cm^{-1} mode of the nanowire and the nanoparticle.

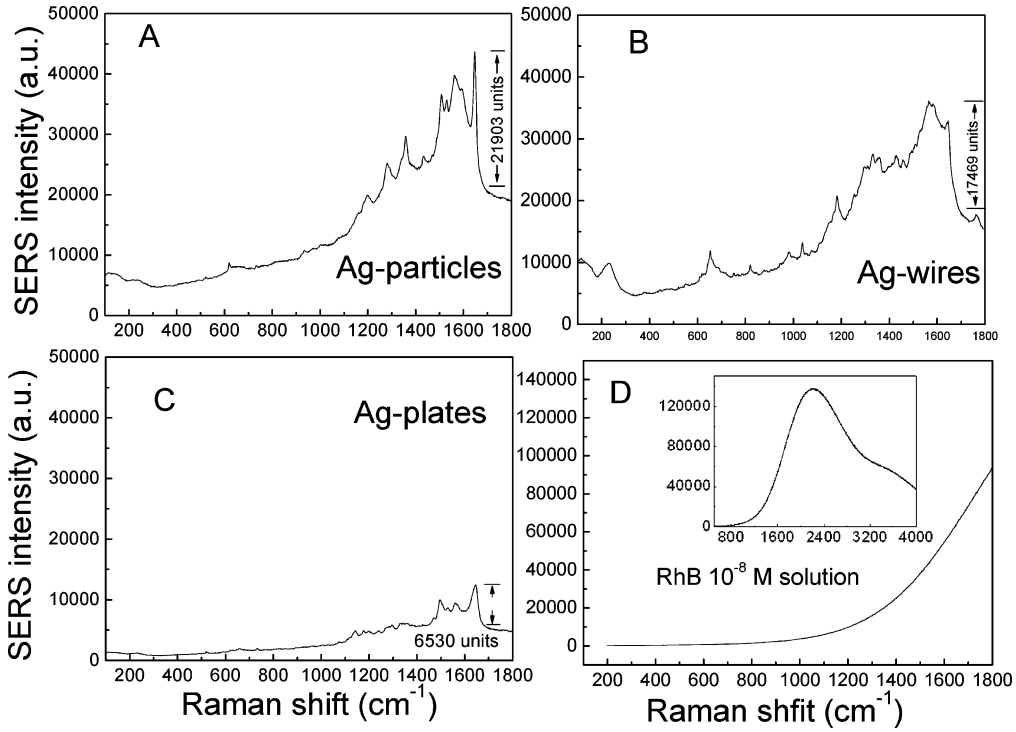

Figure 4. SERS spectral comparison of Ag particle (A), Ag wire (B), and Ag plate (C), using 10^{-8} M rhodamine B (D) dissolved in water. A quantitative enhancement comparison is shown as an inset in figures A−C. The inset in figure D shows the strong fluorescence peak of rhodamine B without the silver enhancement detected under the same Raman parameter. (Excitation power ∼0.47 mW; excitation length 514 nm; charge-coupled device (CCD) detector; 20 times field lens; scan time 10 s; accumulate times 2.)

TABLE 1: Experimental (exptl) and Literature (lit.) SERS Shifts of Rhodamine B Molecules Detected by As-Prepared Ag Substrates

Raman shift				
	exptl			
lit.[28]	Ag particle	Ag wire	Ag plate	assignments[25,29]
1645	1648	1648	1648	aromatic C−C stretching
1595	1595	1595		C═C stretching
1560	1565	1565	1565	aromatic C−C stretching
1525	1529	1529	1529	
1506	1506	1507	1500	aromatic C−C stretching
		1457		
1430	1433	1427	1425	
1356	1356	1360	1352	aromatic C−C streching
		1330	1330	
1275	1280	1294	1290	C−C bridge-bands streching
1195	1201	1185	1200	aromatic C−H bending
		1036		
619	620	650		aromatic bending
233	230	230	230	Ag−N stretching

It is noteworthy that as shown in Figure 4D, without the silver enhancement, there is only the strong fluorescence at ∼2300 cm^{-1} with the intensity three times the SERS enhancement of Figure 4A−C excited by the 514 nm laser. This is reasonable because the maximum absorption wavelength of the RhB molecule is about 540 nm. But when enhanced by as-obtained Ag substrates, the fluorescence energy transfers from the molecules to the metal surface, namely the so-called fluorescence extinction effect.[14] From Table 1, most Raman shifts and the corresponding assignments agree well with the literature reports and only several weak Raman shifts of the nanowire and the nanoplate have no accurate assignments, such as the Raman shifts of 1457, 1330, and 1036 cm^{-1} of the nanowire sample. It also should be noted is that there are several Raman shifts that only appear in nanowire and nanoparticle samples, such as those at 1595 and 620 cm^{-1}, which assigned as the C═C stretching mode and aromatic bending, respectively. This is due to the relatively weaker enhancement of the silver nanoplate.

As shown previously in many reports on SERS, it is widely accepted that the SERS enhancement is the result of a combination of intense localized fields arising from surface plasmon resonance in metallic nanostructures and chemical effects.[9−15] Herein, the SERS enhancements of our samples must also come from both EM and CHEM effects. First, to the EM effects, as-prepared Ag particles have irregular polyhedron morphology with distinct edges and corners; Ag wires have sharp tips and noncircular cross-sections; and Ag plates have sharp angles. Furthermore, as shown in morphology analysis, the crystal faces with high Miller index or with high free energies, such as {110} and {311} crystal faces, easily appear on edges, corners, and protuberances, etc. In good agreement with the "rough surface" electromagnetic enhancement, they can act as "hot sites" for surface plasma. Differing from spherical nanoparticle SERS substrates that rely on interparticle coupling or aggregations, these unconventional nanostructures are considered as independent substrates to enhance the local scattering field. Other nanostructures such as the Langmuir−Blodgett silver nanowire monolayer and crescent moon structures, which have the features of nanotips and sharp edges, have been demonstrated for SERS applications.[12,24] Second, the CHEM effect is also important due to the appearance of Ag−N stretching vibrations at ∼233 cm^{-1} which confirms the RhB molecule is coordinated to the Ag surface through the nonbonding electrons of the nitrogen atom in ethylamino.[25] And then the fluorescence energy of RhB can transfer from the molecules to the metal surface leading to the reduction of the fluorescence intensity and amplification of the Raman enhancement factors.[14]

Considering the weak Raman signal from Ag plate compared with the signals from Ag particle and Ag wire, both the EM effect and CHEM effect should be taken into account. First, the triangular nanoplates are thin and flat. Observing from SEM (Figure 1C), their triangular faces were oriented perpendicular to the Si (100) substrate.[17c] Thus when the incident light of 514 nm was irradiated on the substrate perpendicularly, the Raman signal of RhB produced mainly from the molecule absorbed on the flat face of nanoplates. Second, the surface plasma resonance absorptions of all the as-obtained Ag substrates are away from the 514 nm incident light, which can be seen from Figure 3. Zhang et al. have reported that good metal substrates for SERS must have resonance absorption of incident light.[10]

The CHEM effect, however, should be paid more attention here. As mentioned above, our as-prepared Ag substrates exposed different crystal plates with corresponding well-defined nanostructures. Namely, Ag nanowires mainly exposed {111} and {100} plates known from Figure 1B; whereas the triangular nanoplates exposed nearly {111} plates, which can be seen from diffraction analyses in Figure 1D and the corresponding XRD test. But the nanoparticles have exposed nearly all the crystal faces of FCC silver. Furthermore, just as in the heterogeneous catalysis, the enhanced Raman vibration spectra of organic molecule absorbed at noble metal (Ag colloid, Ag electrode, gold nanoparticle aggregates, et al.) are a surface interaction process.[9a] As the results of previous work, the {110} planes were confirmed more active than {111} and {100} plates in heterogeneous catalysis, which is consistent with the order of free energies associated with these crystallographic planes: $\gamma_{\{110\}} > \gamma_{\{100\}} > \gamma_{\{111\}}$.[26,17]In our work, the sequence of Raman enhancement quality is Ag particle > Ag wire > Ag plate. This is partly due to the exposure of all possible FCC crystal faces in nanoparticles and {100} planes in nanowires that have higher free energies. Their surface atoms are easier to combine with the lone electrons of the RhB molecule. Moreover, the {110} and {311} crystal faces which have higher free energies appear more easily in some particle corners or edges with very small proportions and then act as the "hot site" for chemical absorption. Thus the free energies of crystal planes determine the ability of interaction between surface atoms and organic molecules. Our explanation about the effect of crystal faces can be traced to the last century. Otto et al. had studied the SERS on Cu single-crystal electrodes and concluded that the single-crystal surface, which had a higher Miller index, was more active for SERS enhancing.[27] By far the widely accepted theory on the CHEM effect is charge transfer theory reported by many researchers.[15] Our conclusions here were consistent with this theory. However, our reports put forward the key factor impacting the CHEM enhancement, namely the activity of the exposed crystal plane determines the feasibility and degree of charge transferring between metal atoms and analytes. Of course, theoretical studies as well as further experiments are required to obtain a complete understanding of the CHEM mechanism. But we hope that the present work will stimulate these works.

4. Conclusion

In summary, through different kinds of Ag substrates that have correspondingly particular morphologies and crystal planes, the SERS of rhodamine B dye has been investigated. From the experimental results, we found that the silver substrate, such as nanowire and nanoparticle substrates in this paper, exposed active crystal faces, namely {100}, {110}, and {311} crystal

faces, which had higher free energies and are more favorable for the interaction with organic molecules, and then enhanced the Raman signals by chemical effects. On the other hand, based on the crystal face growth rule, to reach thermodynamic stability, the crystal faces with higher energies should be easier to expose on some edges, corners, etc. with very small proportions, and then they can serve as a "hot site" for surface plasma enhancement. Besides the size effect, the morphology effect is also great for SERS enhancement. It is estimated that this work will contribute to the mechanism of SERS. Moreover, the present results suggest that to improve the Raman enhancement, the SERS metal substrates should expose highly active crystal planes.

Acknowledgment. This work was supported by NSFC (50372030, 20025102, 20131030), the Specialized Research Fund for the Doctoral Program of Higher Education, the Foundation for the Author of National Excellent Doctoral Dissertation of P.R. China, and the State Key Project of Fundamental Research for Nanomaterials and Nanostructures (2003CB716901).

References and Notes

(1) Fleischman, M.; Hendra, P. J.; McQuillan, A. J. *Chem. Phys. Lett.* **1974**, *26*, 123.

(2) Albrecht, M. G.; Creighton, J. A. *J. Am. Chem. Soc.* **1977**, *99*, 5215.

(3) Zhou, D. S.; Xu, N.; Li, L.; Ji, G.; Xue, G. *J. Phys. Chem. B* **2003**, *107*, 2748.

(4) He, P.; Liu, H. T.; Li, Z. Y.; Liu, Y.; Xu, X. D.; Li, J. H. *Langmuir* **2004**, *20*, 10260.

(5) Shafer, K. E.; Haynes, C. L.; Glucksberg, M. R.; Van, R. P. *J. Am. Chem. Soc.* **2003**, *125*, 588.

(6) Yonzon, C. R.; Haynes, C. L.; Zhang, X.; Walsh, J. T.; Van, R. P. *Anal. Chem.* **2004**, *76*, 78.

(7) (a) Nie, S. M.; Emery, S. R. *Science* **1997**, *275*, 1102. (b) Nie, S. M.; Doering W. *J. Phys. Chem. B* **2002**, *106*, 311. (c) Emory, S. R.; Nie, S. M. *J. Phys. Chem. B* **1998**, *102*, 493.

(8) Kneipp, K.; Wang, Y.; Kneipp, H.; Perelman, L. T.; Itzkan, I.; Dasari, R.; Feld, M. S. *Phys. Rev. Lett.* **1997**, *78*, 1667.

(9) (a) Tian, Z. Q.; Ren, B.; Wu, D. Y. *J. Phys. Chem. B* **2002**, *106*, 9463. (b) Ren, B.; Lin, X. F.; Yang, Z. L.; Liu, G. K.; Aroca, R. F.; Mao, B. W.; Tian, Z. Q. *J. Am. Chem. Soc.* **2003**, *125*, 9598.

(10) (a) Grant, C. D.; Schwartzberg, A. M.; Norman, T. J.; Zhang, J. Z. *J. Am. Chem. Soc.* **2003**, *25*, 549. (b) Schwartzberg, A. M.; Grant, C. D.; Wolcott, A.; Talley, C. E.; Huser, T. R.; Bogomolni, R.; Zhang, J. Z. *J. Phys. Chem. B* **2004,** *108*, 19191. (c) (45) Norman, T. J.; Grant, C. D.; Magana, D.; Zhang, J. Z.; Liu, J.; Cao, D. L.; Bridges, F.; Van Buuren, A. *J. Phys. Chem. B* **2002**, *106*, 7005.

(11) Kim, K. L.; Lee, S. J.; Kim, K. *J. Phys. Chem. B* **2004**, *108*, 9216.

(12) Lu, Y.; Liu, G. L.; Kim, J.; Mejia, Y. X.; Lee, L. P. *Nano Lett* **2005**, *5*, 119.

(13) Crozier, K. B.; Sundaramurthy, A.; Kino, G. S.; Quate, C. F. *J. Appl. Phys.* **2003**, *94*, 4632.

(14) Hayazawa, N.; Tarun, A.; Inouye, Y.; Kawata, S. *J. Appl. Phys.* **2002**, *92*, 6983.

(15) Quagliano, L. G. *J. Am. Chem. Soc.* **2004**, *126*, 7393.

(16) (a) Zhou, K. B.; Wang, X.; Sun, X. M.; Peng, Q.; Li, Y. D. *J. Catal.* **2005**, *229*, 206. (b) Zhou, K. B.; Xu, R.; Sun, X. M.; Chen, H. D.; Tian, Q.; Shen, D. X.; Li, Y. D. *Catal. Lett*. Accepted for publication. (c) Wang, X.; Li, Y. D. *J. Am. Chem. Soc.* **2002**, *124*, 2880. (d) Wang, X.; Li, Y. D. *Angew. Chem., Int. Ed.* **2002**, *41*, 4790.

(17) (a) Sun, Y.; Xia, Y. *Science* **2002**, *298*, 2176. (b) Sun, Y.; Xia, Y. *Adv. Mater*. **2002**, *14*, 833. (c) Sun, Y.; Xia, Y. *Adv. Mater*. **2003**, *15*, 695. (d) Sun, Y.; Yin, Y. D.; Mayers, B. T.; Herricks, T.; Xia, Y. *Chem. Mater*. **2002**, *14*, 4736.

(18) (a) Gao, Y.; Jiang, P.; Liu, D. F.; Yuan, H. J.; Yan, X. Q.; Zhou, Z. P.; Wang, J. X.; Song, L.; Liu, L. F.; Zhou, W. Y.; Wang, G.; Wang, C. Y.; Xie, S. S. *Chem. Phys. Lett*. **2003**, *380*, 146. (b) Gao, Y.; Jiang, P.; Liu, D. F.; Yuan, H. J.; Yan, X. Q.; Zhou, Z. P.; Wang, J. X.; Song, L.; Liu, L. F.; Zhou, W. Y.; Wang, G.; Wang, C. Y.; Xie, S. S. *J. Phys. Chem. B* **2004**, *108*, 12877.

(19) (a) Jiang, L. P.; Zhu J. M.; Zhang, J. R.; Zhu J. J.; Chen, H. Y. *Inorg. Chem.* **2004**, *43*, 5877. (b) Chen, S. H.; Carroll, D. L. *Nano Lett.* **2002**, *2*, 1003. (c) Santos, I. P.; Liz-Marzan, L. M. *Nano Lett.* **2002**, *2*, 903.

(20) Yang, P. D. *Nature* **2003**, *425*, 243.

(21) Prywer, J. *J. Cryst. Growth* **2001**, *224*, 134.

(22) (a) Gilman, J. J. *The Art and science of growing crystals*; Wiley: New york, 1963; p 270. (b) Brice, J. C. *J. Cryst. Growth* **1970**, *6*, 205. (c) Min, N. B. *Physical Theory on Crystal Growth*; Shanghai Science and Technology Press: Shanghai, 1982; p 441.

(23) Jin, R. C.; Cao, Y. W.; Mirkin, C. A.; Kelly, K. L.; Schatz, G. C.; Zheng, J. G. *Science* **2001**, *294*, 1901.

(24) Tao, A.; Kim, F.; Hess, C.; Goldberger, J.; He, R.; Sun, Y.; Xia, Y.; Yang, P. D. *Nano Lett.* **2003**, *3*, 1229.

(25) Hildebrandt, P.; Stockburger, M. *J. Phys. Chem. B* **1984**, *88*, 5935.

(26) Wang, Z. L. *J. Phys. Chem. B* **2000**, *104*, 1153.

(27) Otto, A. In *The XVIth International Conference on Raman Spectroscopy*; Heyns, A. M., Ed.; John Wiley & Sons Ltd.: New York, 1998; p 52256.

(28) Wang, G. Z.; Ye, F.; Chao, C.; Zuo, J.; Fang, R. C. *Chin. J. Light Scattering* **1999**, *11*, 142.

(29) Ke, Y. K.; Dong, H. R. *Analytic Chemistry−Spectrum Analysis*; Chemical Industry Press: Beijing, 1998; p 1158.